How to cite: *Angew. Chem. Int. Ed.* **2023,** *62,* e202217023
International Edition: doi.org/10.1002/anie.202217023
German Edition: doi.org/10.1002/ange.202217023

High-pressure Synthesis

Synthesis and Post-Processing of Chemically Homogeneous Nanothreads from 2,5-Furandicarboxylic Acid**

Samuel G. Dunning, Bo Chen, Li Zhu, George D. Cody, Stella Chariton, Vitali B. Prakapenka, Dongzhou Zhang, and Timothy A. Strobel**

Abstract: Compared with conventional, solution-phase approaches, solid-state reaction methods can provide unique access to novel synthetic targets. Nanothreads—one-dimensional diamondoid polymers formed through the compression of small molecules—represent a new class of materials produced via solid-state reactions, however, the formation of chemically homogeneous products with targeted functionalization represents a persistent challenge. Through careful consideration of molecular precursor stacking geometry and functionalization, we report here the scalable synthesis of chemically homogeneous, functionalized nanothreads through the solid-state polymerization of 2,5-furandicarboxylic acid. The resulting product possesses high-density, pendant carboxyl functionalization along both sides of the backbone, enabling new opportunities for the post-synthetic processing and chemical modification of nanothread materials applicable to a broad range of potential applications.

Introduction

While solution-based chemical synthesis is generalizable, controlled organic reactions in the solid state are notoriously challenging due to limitations such as geometrical/steric constraints and multiple energetically competitive pathways.[1] Nevertheless, generalized synthetic control of organic reactions in the solid state with precision comparable to traditional methods would enable a range of new chemical species and synthons that are challenging or impossible to obtain by solution-based chemistry.[2] High-pressure synthesis represents an emerging approach to control solid-state organic transformations that enables novel reactions to produce new structural motifs and novel bonding environments (e.g., sp^3 carbon-rich structures).[3]

Carbon nanothreads are a novel class of one-dimensional sp^3 carbon nanomaterials formed at high pressure. Since the initial formation of diamondoid nanothreads[4] several synthetic strategies have been developed to limit the number of potential reaction pathways and promote the formation of chemically homogeneous products.[3b,5] As the backbones of nanothreads extend in only one direction, these ultrathin carbon materials are predicted to marry the superlative physical properties of diamond with the flexibility of traditional polymers.[6] The chemical composition of nanothreads can be precisely controlled through careful selection of small molecule precursors (e.g., benzene,[4,7] pyridine,[8] pyridazine[5f]), giving them potential advantages over comparable nanomaterials (e.g., nanotubes) for application in varied fields including novel energy storage and advanced structural materials.[6b,9] Nevertheless the formation of chemically homogeneous nanothreads with pristine pendant functionalization remains a significant challenge. Under nanothread-forming conditions, pendant groups can undergo side reactions, resulting in the formation of chemically inhomogeneous, disordered materials that lack specific chemical functionality.[5b,10] A reliable method for synthesizing chemically homogeneous nanothreads with stable functionalization could enable a range of diverse applications including drug discovery,[11] superabsorbent polymers,[12] porous material synthesis,[13] and catalyst design.[14]

As a potential route to produce homogeneous functionalized nanothreads, we investigated π-stacked, heteroatom-substituted aromatics with pendant functionalization and controlled reaction pathways based on molecular crystal structure packing. Furans were selected as the oxygen

[*] S. G. Dunning, G. D. Cody, T. A. Strobel
Earth and Planets Laboratory, Carnegie Institution for Science
Washington, DC-20015 (USA)
E-mail: sdunning@carnegiescience.edu
tstrobel@carnegiescience.edu

B. Chen
Donostia International Physics Center
Paseo Manuel de Lardizabal, 4, 20018 Donostia-San Sebastian (Spain)

B. Chen
IKERBASQUE, Basque Foundation for Science
Plaza Euskadi 5, 48009 Bilbao (Spain)

L. Zhu
Physics Department, Rutgers University-Newark
101 Warren Street, Newark, NJ-07102 (USA)

S. Chariton, V. B. Prakapenka
Center for Advanced Radiation Sources, The University of Chicago
Chicago, IL-60637 (USA)

D. Zhang
Hawaii Institute of Geophysics and Planetology, School of Ocean and Earth Science and Technology, University of Hawaii at Manoa
Honolulu, HI-96822 (USA)

[**] A previous version of this manuscript has been deposited on a preprint server (https://doi.org/10.26434/chemrxiv-2022-45nt5).

heteroatom substitution reduces aromaticity and can guide nanothread formation along a carbon-exclusive reaction pathway, resulting in the formation of so-called "perfect" nanothreads.[5c,d] Functional groups containing hydrogen bond donors/acceptors were chosen due to the strength of hydrogen-bonding interactions,[15] which we hypothesized would stabilize the geometry under compression and minimize potential intermolecular side reactions. Following this approach, we report here the synthesis and characterization of a chemically homogeneous crystalline nanothread polymer, formed by the compression of 2,5-furandicarboxylic acid (2,5-FDCA). The resulting carboxyl-rich product is among the first pristine, homogeneous pendant-functionalized nanothreads, and presents new opportunities for the post-processing of nanothread materials, including small molecule adsorption and metal binding.

Results and Discussion

2,5-furandicarboxylic acid crystallizes[16] with molecular π-stacking suitable for a topochemical-type reaction pathway under compression (i.e., $d_c < \approx 4$ Å, $\Phi \approx 25°$, see Figure 1).[5f,10] The ambient-pressure, closest-contact intermolecular C–C distances of 3.28 Å indicate that the system is a likely candidate to undergo a nanothread-forming intermolecular [4+2] cycloaddition reaction, consistent with the known mechanism for furan nanothread formation as determined by solid-state NMR studies.[5c] While pendant functional groups can cause unwanted side reactions resulting in the formation of chemically inhomogeneous products, the carboxyl groups in 2,5-FDCA are stabilized in a hydrogen-bonding network, which may help preserve homogeneous functionalization during cycloaddition along the carbon backbone.

To examine this reaction pathway experimentally, ground powders and single-crystals of 2,5-FDCA were loaded into diamond anvil cells (DACs) and compressed to pressures up to 30 GPa while the structure and bonding was monitored in situ using a combination of X-ray diffraction (XRD) and vibrational spectroscopy. XRD patterns from powder samples agree with the known molecular structure and were readily indexed to a monoclinic $P2_1/m$ cell (Figure 1D).[16] During compression, diffraction peaks shift to lower *d*-spacings caused by the pressure-induced contraction of the unit cell (Figure S1). Above 13 GPa, a 9 % drop in the unit cell volume, associated with a large decrease in the molecular stacking direction (*c*-axis), indicates the onset of nanothread formation (Figure 1). Simultaneously, the sample transforms to an orange color, which was previously associated with nanothread polymerization.[5a,e,f,8] Decreased compressibility observed at higher pressures is indicative of a denser covalent nanothread material. Single-crystal diffraction measurements of 2,5-FDCA are in good agreement with the powder data and show a clear splitting of Bragg peaks with the same symmetry indicating a polymerization-induced, single-crystal-to-single-crystal transformation (Figure S2).

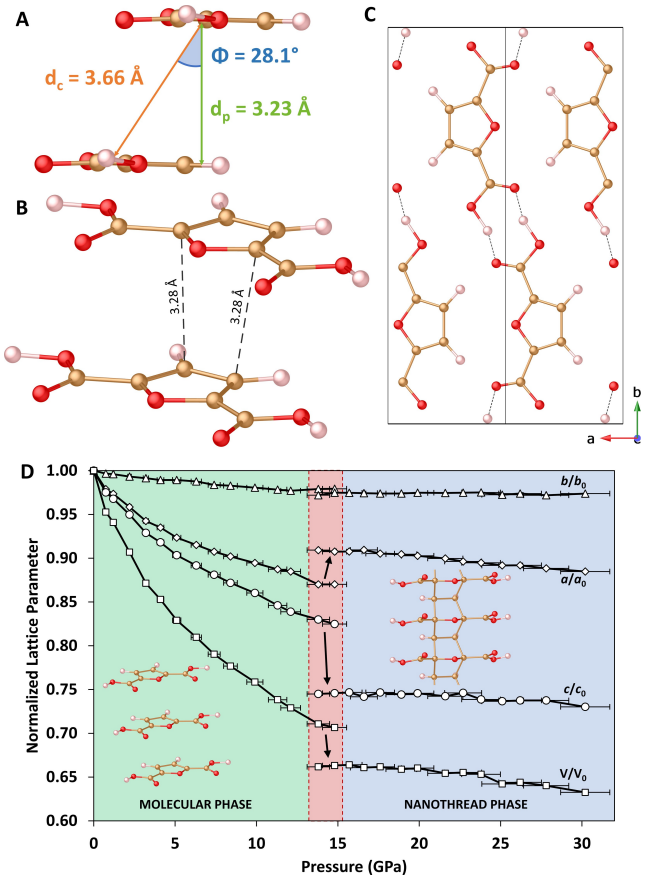

Figure 1. A) Starting molecular structure of 2,5-furandicarboxylic acid (2,5-FDCA) showing local π-stacking at ambient conditions. d_c is the centroid distance between rings, d_p is the distance between parallel planes, ϕ is the slippage angle between ring centroids, defined by the ring normal and centroid vectors; B) Nearest-neighbor [4+2] cycloaddition pathway; C) View of 2,5-FDCA along the molecular stacking c-axis; D) Comparison of relative changes in unit cell parameters as a function of pressure.

In situ FTIR measurements show the clear onset of a chemical reaction near 13 GPa, confirming that the changes observed by XRD are due to nanothread formation. The FTIR spectrum of 2,5-FDCA collected at low pressure is in good agreement with previous studies, and no low-pressure, polymorphic phase transitions occur under compression.[17] Above ≈14 GPa, several new peaks at *ca.* 1163, 1103, 899, and 717 cm^{-1} appear, followed by additional peaks at ca. 1510 and 1282 cm^{-1} above 17 GPa. Across the same pressure range, peaks corresponding to sp^2 C=C and C–H vibrations decrease dramatically in intensity, disappearing entirely above 19 GPa (Figure S3). In situ Raman spectra (Figure S4) indicate the sample becomes sensitive to laser damage above 5 GPa and shows a loss of molecular vibrational modes above the reaction onset pressure, consistent with previously reported nanothread materials.[5f,8]

PXRD of the recovered product (Figure 2A) shows similar features as the original molecular lattice of 2,5-FDCA, but with significantly shifted peaks caused by nanothread formation. The preservation of crystalline long-range

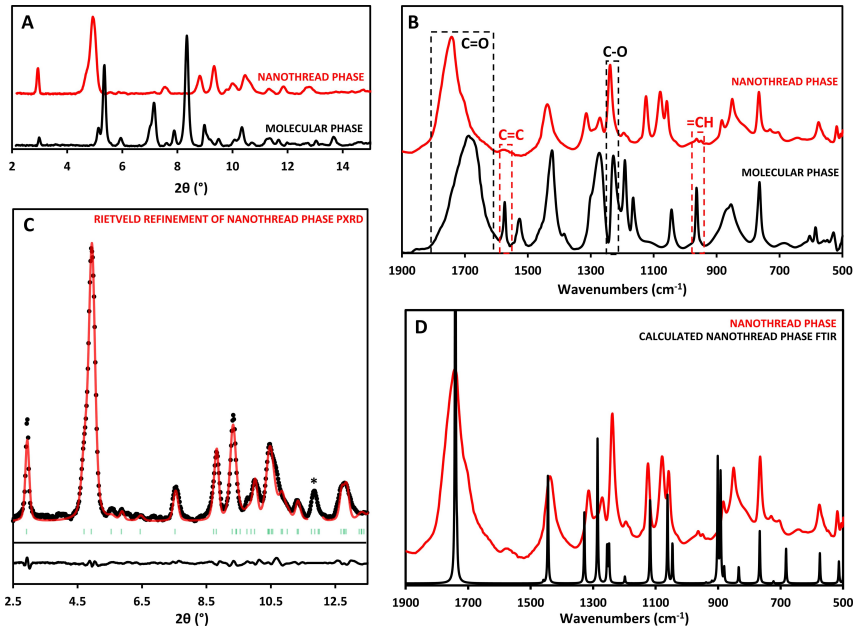

Figure 2. A) Comparison of the integrated 1D XRD patterns at 1 atm for molecular 2,5-FDCA (black), and the nanothread phase recovered from 30 GPa (red), $\lambda = 0.4340$ Å; B) Comparison of the FTIR spectra at 1 atm for molecular 2,5-FDCA (black) and the nanothread phase recovered from 24.5 GPa (red). Red boxes indicate peaks corresponding to sp^2 C=C or C–H vibrations which disappear after reaction. Black boxes indicate vibrations corresponding to carboxyl C=O and C–O vibrations, which remain in the nanothread; C) XRD pattern of *syn*-2,5-FDCA nanothreads at 1 atm (black points) with Rietveld refinement (red line), $\lambda = 0.4340$ Å. The asterisk (*) indicates scattering from the Re gasket and has been excluded from refinement; D) Comparison of the experimental FTIR spectrum of *syn*-2,5-FDCA at 1 atm (red), and the calculated (B3LYP) FTIR spectrum for the DFT-optimized structure of *syn*-2,5-FDCA (black). Calculated frequencies, shown by arbitrary Lorentzian peak widths, were scaled by 0.98 to match the highest intensity peak.

order to *d*-spacings below 2 Å upon decompression is in contrast to furan nanothreads.[5c,d] We hypothesize that the improved stacking relative to molecular furan and the enhanced stability provided by the hydrogen bonding network in 2,5-FDCA prevents structural rearrangement of the resulting nanothread polymer. The FTIR spectrum of the recovered material (Figure 2B) also indicates a high degree of chemical homogeneity, exhibiting sharp, well-defined absorption features. Importantly, the presence of absorption bands at ca. 1742 and 1238 cm^{-1}, due to carboxyl C=O and C–O vibrations, respectively, confirm retention of the carboxylic acid groups on the recovered nanothread. Notably, the shift in the C=O vibration to higher frequency indicates a change in the attached furan ring from an unsaturated to a saturated hydrocarbon, further confirming nanothread formation.[18] Ordered carboxyl O–H vibrations at ca. 3151 and 3125 cm^{-1} also shift to a broader singlet at ca. 3054 cm^{-1} indicating retention of the hydrogen bonding network between the resulting nanothreads (Figure S3). Due to the broad –OH vibrations above 3000 cm^{-1}, sp^3 C–H stretching vibrations cannot be used to identify a nanothread-forming reaction. However, loss of the sp^2 C=C and C–H vibrations at ca. 1572 cm^{-1} and 962 cm^{-1} in the recovered material demonstrate a change in the hybridization of the furan carbon backbone due to nanothread formation.

To further understand the structure of the recovered polymer we optimized packed *syn*-2,5-FDCA nanothreads using density functional theory (DFT) for direct comparison of experimental observables with calculated data (Figure 2). While furan nanothreads have been found to form in the *anti*-conformation[5c,d] (i.e., oxygens alternate sides along the nanothread backbone) 2,5-FDCA forms nanothreads in the *syn* conformation based on the stacking of molecular 2,5-FDCA (i.e., all oxygen atoms aligned along one side of the molecular stack). The calculated FTIR spectrum of the *syn* polymer (hereafter referred to as *syn*-2,5-FDCA) is in excellent agreement with experiment (Figure 2D), allowing for the unambiguous assignment of the spectrum (Table S1). For example, new peaks at 1271 and 1238 cm^{-1} represent sp^3 C–H wagging and sp^3 C–H bending vibrations, respectively, that are diagnostic of nanothread formation. Similarly, Rietveld refinement of the diffraction pattern starting from the DFT-optimized model confirms the structure of the nanothread (Figures 2C & 3A). The recovered structure was refined in a monoclinic lattice with cell parameters: $a = 5.265(4)$ Å, $b = 16.918(5)$ Å, $c = 2.670(4)$ Å, and $\beta = 90.28(5)°$ (see Tables S2&S3), in good agreement with a similar study published while this manuscript was under review.[19] Furthermore, solid-state ^{13}C NMR of a sample synthesized in a Paris-Edinburgh (PE) press shows six well-resolved peaks at 167, 165, 146, 124, 89 and 58 ppm (Figure 3B). The sharp peaks at 165, 146 and 124 ppm originate from residual 2,5-FDCA. The remaining broader peaks at 167, 89 and 58 ppm from the nanothread are assigned to sp^2 COOH, sp^3 O–C–COOH and sp^3 C–H, respectively. Methanol washing was found to successfully remove residual starting material,

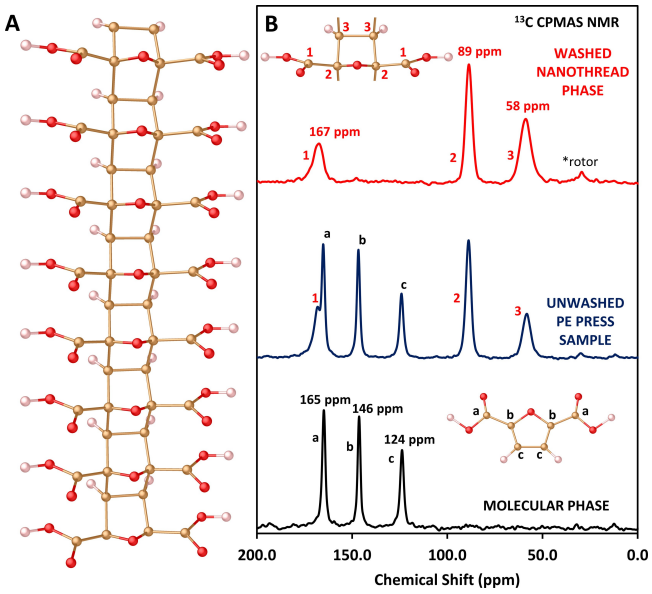

Figure 3. A) Structure of the nanothread polymer, *syn*-2,5-FDCA, containing 8 repeat units.; B) Comparison of the solid-state ^{13}C CPMAS NMR spectra for 2,5-FDCA (black), an unwashed PE press sample (blue) containing unreacted starting material and nanothread phase (see inset structural images for assignments), and a washed PE press sample (red).

providing a simple route to obtain the pure, chemically homogeneous nanothread product.

This chemically homogeneous, densely functionalized nanothread polymer represents a new kind of hydrogen-bonded organic framework (HOF) material.[20] HOFs are currently of broad interest due to their simple synthesis procedures and unique gas uptake properties. Similar HOFs and other carboxyl-rich polymers such as poly(acrylic acid) are known to have unique sorption properties (e.g., superabsorbent water uptake), and indeed, *syn*-2,5-FDCA nanothreads immediately absorb moisture when exposed to ambient air. This water absorption is accompanied by a color change from orange to white along with significant volume swelling of the material, loss of crystallinity and new FTIR absorption bands associated with water uptake and loss of periodic ordering between nanothreads (Figure S5–S7). Solid-state ^{13}C NMR measurements, demonstrate that no chemical changes occur to the nanothread backbone upon hydration. The hygroscopic nature of the sample was confirmed by thermogravimetric analysis (TGA) which shows an initial mass loss below 100 °C characteristic of the loss of weakly sorbed water. TGA analysis also shows a sharp 74.6 % mass loss starting at 282 °C, indicating the onset of thermal decomposition, consistant with the molecular phase (Figure 4C). Preliminary water sorption capacity studies carried out using the tea-bag method[21] reveal that *syn*-2,5-FDCA increases in mass by 174 % after 10 minutes of direct water exposure. The hydrophilic nature of this material warrants additional investigation for the sorption of other small molecules and opens the possibility for novel separation and storage applications using functionalized nanothreads.

In addition to sorption properties enabled by functionalized nanothread surfaces, *syn*-2,5-FDCA opens new explorations of more complex post-synthetic reactivity, which could be used to precisely tune chemical and physical properties across diverse applications including nanothread-based nanoparticle/catalyst supports,[22] chemical sensors,[23] and the formation extended porous structures such as metal–organic frameworks (MOFs)[24] with nanothread linkers. Recent theoretical studies indicate that doping nanothreads with 3*d* transition metals can significantly alter their electronic and magenetic properties,[25] however the incorporation of metals into nanothread systems has not been demonstrated experimentally. The hygroscopic nature of *syn*-2,5-FDCA indicates the carboxylates in this material are

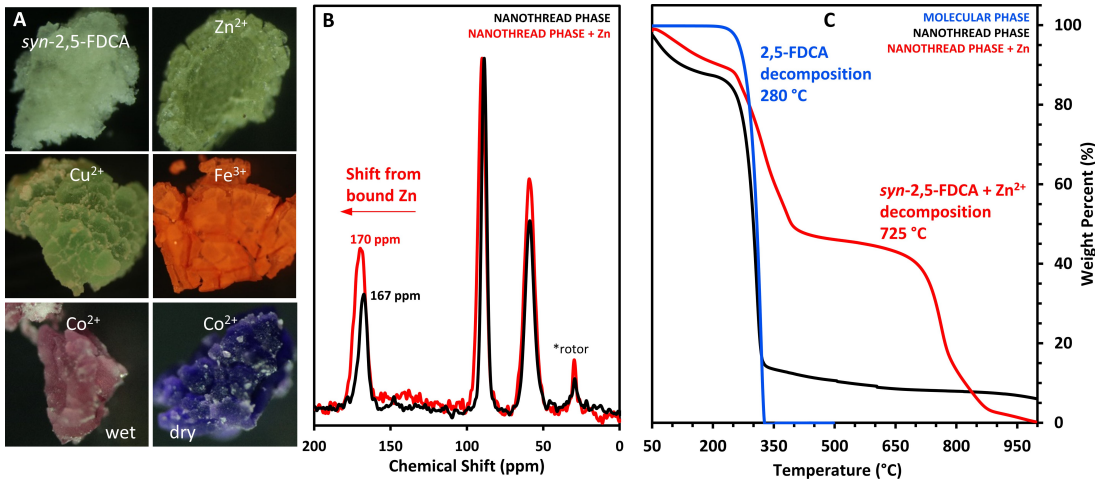

Figure 4. A) Reflected-light images showing samples of hydrated *syn*-2,5-FDCA before and after exposure to a variety of metal cations; B) Comparison of the solid-state ^{13}C CPMAS NMR spectra for *syn*-2,5-FDCA before (black) and after exposure to Zn^{2+} cations (red). Note the shift in the COOH peak from 167 to 170 ppm indicating Zn binding; C) Comparison of the TGA curves for 2,5-FDCA (blue), *syn*-2,5-FDCA (black), and *syn*-2,5-FDCA-Zn (red).

chemically accessible for reactions such as metal binding. In order to test the feasibility of producing metal-bound nanothread structures, samples of *syn*-2,5-FDCA were deprotonated and exposed to a variety of 3*d* transition metals (Fe^{3+}, Co^{2+}, Cu^{2+}, Zn^{2+}) that are commonly used in MOF formation, and have been shown to readily bind to acid-rich polymers such as poly(acrylic acid).[26] Samples exposed to Fe^{3+}, Co^{2+}, and Cu^{2+} all show distinct color changes that persist after multiple washes, indicating permanent metal coordination (Figure 4A). Solid-state ^{13}C NMR collected on the sample exposed to Zn^{2+} shows a shift in the carboxyl peak to 170 ppm (Figure 4B), consistent with a carboxylate bound to a d^{10} metal (*cf.* 172 ppm in MOF-5 (Zn),[27] 171 ppm in UiO-66 (Zr)[28]). Such a change in the NMR spectrum of *syn*-2,5-FDCA confirms successful metal binding to the nanothread backbone. TGA of the same material exhibits two sharp decomposition features. The first, with onset of 280 °C, is consistent with thermal decomposition reactions, including decarboxylation of free –COOH groups (Figure 4C).[29] This initial decomposition is then followed by a region of stability between 380–725 °C after which a second decomposition event is observed. Similar TGA curves are commonly seen in materials rich in metal-carboxylate interactions (e.g., MOFs).[30] TGA curves of the other metalated threads showed similar changes in the shape and onset temperature of thermal decomposition upon metal coordination (Figure S8). These results indicate that a wide range of metals may bind to the nanothread backbone.

The metallation process of *syn*-2,5-FDCA results in amorphous products, so the precise nature of metal binding from a crystallographic structure is currently unknown. However, the case of *syn*-2,5-FDCA-Co clearly reveals the presence of open metal sites via reversible pink/blue color changes related to changes in local coordination geometry.[31] These materials are being investigated further for their use as a new class of sorbent polymers, given that systems with open metal sites have been shown to possess unique and unusual gas sorption and chemical sensing properties.[32] The successful incorproation of metals into *syn*-2,5-FDCA represents an important proof-of-concept for the development of transition metals into nanothread systems, and opens the door to the possibility of using nanothreads as independent synthons for the formation of more complex frameworks (i.e., MOFs), as chemically robust support materials, and other advanced applications.

Conclusion

In conclusion, we have shown how careful consideration of molecular stacking geometry and functionality can be used to produce chemically homogeneous, functionalized nanothread polymers via pressure-induced polymerization. Compression of 2,5-furandicarboxylic acid to approximately 13 GPa induces a series of constrained [4+2] Diels-Alder cycloaddition reactions, resulting in a chemically homogeneous sp^3 furan backbone polymer that is functionalized with a high density of carboxyl groups. This nanothread exhibits potential superabsorbent properties, readily absorbing ambient moisture. In addition, the pendant functionalization enables the coordination of various 3*d* metal ions suggesting the possibility for functionalized nanothreads to act as a novel class of synthons. These results signify the first example of deliberate, controlled *post*-synthetic modification of a nanothread, which may ultimately lead to the development of extended nanothread-based networks with a wide range of novel physical properties.

Acknowledgements

Portions of this work were performed at GeoSoilEnviroCARS (The University of Chicago, Sector 13) Advanced Photon Source (APS), Argonne National Laboratory. GeoSoilEnviroCARS is supported by the National Science Foundation - Earth Sciences (EAR-1634415) and Department of Energy—GeoSciences (DE-FG02-94ER14466). This research used resources of the Advanced Photon Source; a U.S. Department of Energy (DOE) Office of Science User Facility operated for the DOE Office of Science by Argonne National Laboratory under Contract DE-AC02-06CH11357.

The authors acknowledge funding support from The Arnold and Mabel Beckman Foundation (Arnold O. Beckman Postdoctoral Fellowship in Chemical Sciences Program) and the U.S. Army Research Office (Grant W911NF-17-1-0604).

The authors would like to acknowledge Dr. Timothy Mock (Carnegie Institution for Science) for his assistance in collecting ICP-MS data.

Conflict of Interest

The authors declare no conflict of interest.

Data Availability Statement

The data that support the findings of this study are available from the corresponding author upon reasonable request.

Keywords: Carbon Nanomaterials · High Pressure · Hydrogen Bonded Organic Frameworks · Nanothreads

[1] a) S. E. Rodil, A. C. Ferrari, J. Robertson, W. I. Milne, *J. Appl. Phys.* **2001**, *89*, 5425–5430; b) M. Citroni, S. Fanetti, C. Bazzicalupi, K. Dziubek, M. Pagliai, M. M. Nobrega, M. Mezouar, R. Bini, *J. Phys. Chem. C* **2015**, *119*, 28560–28569; c) T. S. Zhu, E. Ertekin, *Nano Lett.* **2016**, *16*, 4763–4772; d) H. Y. Gou, B. L. Yonke, A. Epshteyn, D. Y. Kim, J. S. Smith, T. A. Strobel, *J. Chem. Phys.* **2015**, *142*, 194503; e) D. W. Keefer, H. Y. Gou, A. P. Purdy, A. Epshteyn, D. Young, J. V. Badding, T. A. Strobel, *J. Phys. Chem. A* **2016**, *120*, 9370–9377; f) D. W. Keefer, H. Y. Gou, Q. Q. Wang, A.

Purdy, A. Epshteyn, S. J. Juhl, G. D. Cody, J. Badding, T. A. Strobel, *J. Phys. Chem. A* **2018**, *122*, 2858–2863; g) F. Li, J. Xu, Y. Wang, H. Zheng, K. Li, *Molecules* **2021**, *26*, 7581; h) X. Yang, X. Wang, Y. Wang, K. Li, H. Zheng, *Crystals* **2019**, *9*, 490; i) K. Biradha, R. Santra, *Chem. Soc. Rev.* **2013**, *42*, 950–967; j) G. Kaupp in *Encyclopedia of Physical Organic Chemistry* (Ed.: Z. Wang), Wiley, Hoboken, **2016**, pp. 1–80; k) J. M. Thomas, *Philos. Trans. R. Soc. London Ser. A* **1974**, *277*, 251–286; l) G. Wegner, *Makromol. Chem.* **1972**, *154*, 35–48; m) G. Wegner, *Pure Appl. Chem.* **1977**, *49*, 443–454; n) V. Enkelmann in *Polydiacetylenes* (Ed.: H.-J. Cantow), Springer Berlin Heidelberg, Berlin, **1984**, pp. 91–136; o) R. H. Baughman, *J. Appl. Phys.* **1972**, *43*, 4362–4370.

[2] G.-W. Wang, *Chem. Soc. Rev.* **2013**, *42*, 7668–7700.

[3] a) M. D. Ward, H. T. Huang, L. Zhu, D. Popov, T. A. Strobel, *J. Phys. Chem. C* **2019**, *123*, 11369–11377; b) H. T. Huang, L. Zhu, M. D. Ward, T. Wang, B. Chen, B. L. Chaloux, Q. Q. Wang, A. Biswas, J. L. Gray, B. Kuei, G. D. Cody, A. Epshteyn, V. H. Crespi, J. V. Badding, T. A. Strobel, *J. Am. Chem. Soc.* **2020**, *142*, 17944–17955; c) S. Romi, S. Fanetti, F. Alabarse, R. Bini, *J. Phys. Chem. C* **2021**, *125*, 17174–17182; d) S. Romi, S. Fanetti, F. G. Alabarse, R. Bini, M. Santoro, *Chem. Mater.* **2022**, *34*, 2422–2428; e) S. Romi, S. Fanetti, F. Alabarse, A. M. Mio, J. Haines, R. Bini, *Nanoscale* **2022**, *14*, 4614–4625; f) L. Zhu, G. M. Borstad, H. Liu, P. A. Guńka, M. Guerette, J.-A. Dolyniuk, Y. Meng, E. Greenberg, V. B. Prakapenka, B. L. Chaloux, A. Epshteyn, R. E. Cohen, T. A. Strobel, *Sci. Adv.* **2020**, *6*, eaay8361; g) P. Duan, X. Li, T. Wang, B. Chen, S. J. Juhl, D. Koeplinger, V. H. Crespi, J. V. Badding, K. Schmidt-Rohr, *J. Am. Chem. Soc.* **2018**, *140*, 7658–7666; h) T. B. Shiell, C. de Tomas, D. G. McCulloch, D. R. McKenzie, A. Basu, I. Suarez-Martinez, N. A. Marks, R. Boehler, B. Haberl, J. E. Bradby, *Phys. Rev. B* **2019**, *99*, 024114; i) C.-S. Yoo, *Matter Radiat. Extremes* **2020**, *5*, 018202; j) C.-S. Yoo, M. Kim, J. Lim, Y. J. Ryu, I. G. Batyrev, *J. Phys. Chem. C* **2018**, *122*, 13054–13060; k) R. Bini, V. Schettino, *Materials under extreme conditions molecular crystals at high pressure*, Imperial College Press, London, **2014**; l) K. Aoki, Y. Kakudate, M. Yoshida, S. Usuba, K. Tanaka, S. Fujiwara, *Synth. Met.* **1989**, *28*, D91–D98; m) J. V. Badding, L. J. Parker, D. C. Nesting, *J. Solid State Chem.* **1995**, *117*, 229–235; n) V. C. Bastron, H. G. Drickamer, *J. Solid State Chem.* **1971**, *3*, 550–563; o) W. Grochala, R. Hoffmann, J. Feng, N. W. Ashcroft, *Angew. Chem. Int. Ed.* **2007**, *46*, 3620–3642; *Angew. Chem.* **2007**, *119*, 3694–3717; p) B. Chen, R. Hoffmann, R. Cammi, *Angew. Chem. Int. Ed.* **2017**, *56*, 11126–11142; *Angew. Chem.* **2017**, *129*, 11278–11295; q) V. V. Brazhkin, *High Pressure Res.* **2007**, *27*, 333–351; r) R. Bini, M. Ceppatelli, M. Citroni, V. Schettino, *Chem. Phys.* **2012**, *398*, 262–268; s) P. F. McMillan, *Nat. Mater.* **2002**, *1*, 19–25.

[4] T. C. Fitzgibbons, M. Guthrie, E. S. Xu, V. H. Crespi, S. K. Davidowski, G. D. Cody, N. Alem, J. V. Badding, *Nat. Mater.* **2015**, *14*, 43–47.

[5] a) M. D. Ward, W. S. Tang, L. Zhu, D. Popov, G. D. Cody, T. A. Strobel, *Macromolecules* **2019**, *52*, 7557–7563; b) M. C. Gerthoffer, S. K. Wu, B. Chen, T. Wang, S. Huss, S. M. Oburn, V. H. Crespi, J. V. Badding, E. Elacqua, *Chem. Sci.* **2020**, *11*, 11419–11424; c) B. S. Matsuura, S. Huss, Z. X. Zheng, S. C. Yuan, T. Wang, B. Chen, J. V. Badding, D. Trauner, E. Elacqua, A. C. T. van Duin, V. H. Crespi, K. Schmidt-Rohr, *J. Am. Chem. Soc.* **2021**, *143*, 9529–9542; d) S. Huss, S. K. Wu, B. Chen, T. Wang, M. C. Gerthoffer, D. J. Ryan, S. E. Smith, V. H. Crespi, J. V. Badding, E. Elacqua, *ACS Nano* **2021**, *15*, 4134–4143; e) A. Biswas, M. D. Ward, T. Wang, L. Zhu, H. T. Huang, J. V. Badding, V. H. Crespi, T. A. Strobel, *J. Phys. Chem. Lett.* **2019**, *10*, 7164–7171; f) S. G. Dunning, L. Zhu, B. Chen, S. Chariton, V. B. Prakapenka, M. Somayazulu, T. A. Strobel, *J. Am. Chem. Soc.* **2022**, *144*, 2073–2078; g) D. Gao, X. Tang, J. Xu, X. Yang, P. Zhang, G. Che, Y. Wang, Y. Chen, X. Gao, X. Dong, H. Zheng, K. Li, H.-k. Mao, *Proc. Natl. Acad. Sci. USA* **2022**, *119*, e2201165119.

[6] a) H. F. Zhan, Y. T. Gu in *Thermal Transport in Carbon-Based Nanomaterials* (Ed.: G. Zhang), Elsevier, Amsterdam, **2017**, pp. 185–204; b) J. Silveira, A. R. Muniz, *Carbon* **2017**, *113*, 260–265; c) L. W. Zhang, W. M. Ji, K. M. Liew, *Carbon* **2018**, *132*, 232–240; d) H. F. Zhan, Y. T. Gu, *Chin. Phys. B* **2018**, *27*, 038103; e) Y. X. Xue, Y. Chen, Z. Li, J. W. Jiang, Y. Y. Zhang, N. Wei, *J. Phys. D* **2019**, *52*, 085301; f) P. Wang, H. F. Zhan, Y. T. Gu, *ACS Appl. Nano Mater.* **2020**, *3*, 10218–10225.

[7] X. Li, M. Baldin, T. Wang, B. Chen, E. S. Xu, B. Vermilyea, V. H. Crespi, R. Hoffmann, J. J. Molaison, C. A. Tulk, M. Guthrie, S. Sinogeikin, J. V. Badding, *J. Am. Chem. Soc.* **2017**, *139*, 16343–16349.

[8] X. Li, T. Wang, P. Duan, M. Baldini, H. T. Huang, B. Chen, S. J. Juhl, D. Koeplinger, V. H. Crespi, K. Schmidt-Rohr, R. Hoffmann, N. Alem, M. Guthrie, X. Zhang, J. V. Badding, *J. Am. Chem. Soc.* **2018**, *140*, 4969–4972.

[9] a) R. E. Roman, K. Kwan, S. W. Cranford, *Nano Lett.* **2015**, *15*, 1585–1590; b) H. F. Zhan, G. Zhang, V. B. C. Tan, Y. Cheng, J. M. Bell, Y. W. Zhang, Y. T. Gu, *Nanoscale* **2016**, *8*, 11177–11184.

[10] W. S. Tang, T. A. Strobel, *J. Phys. Chem. C* **2020**, *124*, 25062–25070.

[11] C. Ballatore, D. M. Huryn, A. B. Smith III, *ChemMedChem* **2013**, *8*, 385–395.

[12] J. Zohuriaan, K. Kabiri, *Iran. Polym. J.* **2008**, *17*, 451–477.

[13] H.-C. Zhou, J. R. Long, O. M. Yaghi, *Chem. Rev.* **2012**, *112*, 673–674.

[14] Z. Zhu, M. Odagi, N. Supantanapong, W. Xu, J. Saame, H.-U. Kirm, K. A. Abboud, I. Leito, D. Seidel, *J. Am. Chem. Soc.* **2020**, *142*, 15252–15258.

[15] S. C. C. van der Lubbe, C. F. Guerra, *Chem. Asian J.* **2019**, *14*, 2760–2769.

[16] E. Martuscelli, C. Pedone, *Acta Crystallogr. Sect. B* **1968**, *24*, 175–179.

[17] S. Zhang, L. Zhang, *Pol. J. Chem. Technol.* **2017**, *19*, 11–16.

[18] W. E. W. NIST Mass Spectrometry Data Center, director, in *NIST Chemistry WebBook, NIST Standard Reference Database Number 69* (Ed.: P. J. L. a. W. G. Mallard), National Institute of Standards and Technology, Gaithersburg MD, 20899.

[19] X. Wang, X. Yang, Y. Wang, X. Tang, H. Zheng, P. Zhang, D. Gao, G. Che, Z. Wang, A. Guan, J.-F. Xiang, M. Tang, X. Dong, K. Li, H.-k. Mao, *J. Am. Chem. Soc.* **2022**, *144*, 21837–21842.

[20] P. Li, M. R. Ryder, J. F. Stoddart, *Acc. Mater. Res.* **2020**, *1*, 77–87.

[21] a) K. Zhang, W. Feng, C. Jin, *MethodsX* **2020**, *7*, 100779; b) V. Poornima, R. Venkatasubramani, V. Sreevidya, V. Vignesh, K. Adithan, *IOP Conf. Ser.: Mater. Sci. Eng.* **2020**, *872*, 012174.

[22] a) H.-J. Tang, T.-T. Han, Z.-J. Luo, X.-Y. Wu, *Chin. Chem. Lett.* **2013**, *24*, 63–66; b) Z. Luo, L. Qu, T. Han, Z. Zhang, X. Shao, X. Wu, Z.-l. Chen, *Eur. J. Inorg. Chem.* **2014**, 994–1000; c) L. Qu, D. Huang, H. Shi, M. Gu, J. Li, F. Dong, Z. Luo, *J. Phys. Chem. Solids* **2015**, *85*, 173–179.

[23] a) H. Tan, S.-Y. Park, *ACS Sens.* **2021**, *6*, 1039–1048; b) C. Song, Q. Song, Z. Ding, Y. Han, *Nanomaterials* **2022**, *12*, 2398.

[24] a) H. Furukawa, K. E. Cordova, M. O'Keeffe, O. M. Yaghi, *Science* **2013**, *341*, 1230444; b) S. Mandal, S. Natarajan, P. Mani, A. Pankajakshan, *Adv. Funct. Mater.* **2021**, *31*, 2006291; c) Z. Zhang, H. T. H. Nguyen, S. A. Miller, S. M. Cohen, *Angew. Chem. Int. Ed.* **2015**, *54*, 6152–6157; *Angew. Chem.* **2015**, *127*, 6250–6255.

[25] Z. Z. Miao, C. Cao, B. Zhang, H. M. Duan, M. Q. Long, *Chin. Phys. B* **2020**, *29*, 066101.

[26] a) F. T. Wall, S. J. Gill, *J. Phys. Chem.* **1954**, *58*, 1128–1130; b) M. R. Shaik, M. Kuniyil, M. Khan, N. Ahmad, A. Al-Warthan, M. R. H. Siddiqui, S. F. Adil, *Molecules* **2016**, *21*, 292; c) S. Moulay, N. Bensacia, *Int. J. Ind. Chem.* **2016**, *7*, 369–389; d) A. S. Chevtaev, A. I. Tabunshchikov, A. S. Ozerin, F. S. Radchenko, I. A. Novakov, *Russ. J. Gen. Chem.* **2020**, *90*, 870–873.

[27] S. Bennabi, M. Belbachir, *J. Mater. Environ. Sci.* **2017**, *8*, 4391–4398.

[28] S. Devautour-Vinot, G. Maurin, C. Serre, P. Horcajada, D. Paula da Cunha, V. Guillerm, E. de Souza Costa, F. Taulelle, C. Martineau, *Chem. Mater.* **2012**, *24*, 2168–2177.

[29] a) G. R. Dick, A. D. Frankhouser, A. Banerjee, M. W. Kanan, *Green Chem.* **2017**, *19*, 2966–2972; b) B. R. Brown, *Q. Rev. Chem. Soc.* **1951**, *5*, 131–146.

[30] J. H. Cavka, S. Jakobsen, U. Olsbye, N. Guillou, C. Lamberti, S. Bordiga, K. P. Lillerud, *J. Am. Chem. Soc.* **2008**, *130*, 13850–13851.

[31] a) S. Ghosh, S. Kamilya, M. Das, S. Mehta, M.-E. Boulon, I. Nemec, M. Rouzières, R. Herchel, A. Mondal, *Inorg. Chem.* **2020**, *59*, 7067–7081; b) J. Ren, T. Lin, L. W. Sprague, I. Peng, L.-Q. Wang, *J. Chem. Educ.* **2020**, *97*, 509–516.

[32] a) Y.-W. Li, J.-R. Li, L.-F. Wang, B.-Y. Zhou, Q. Chen, X.-H. Bu, *J. Mater. Chem. A* **2013**, *1*, 495–499; b) J. J. Perry, S. L. Teich-McGoldrick, S. T. Meek, J. A. Greathouse, M. Haranczyk, M. D. Allendorf, *J. Phys. Chem. C* **2014**, *118*, 11685–11698; c) S. G. Dunning, A. J. Nunez, M. D. Moore, A. Steiner, V. M. Lynch, J. L. Sessler, B. J. Holliday, S. M. Humphrey, *Chem* **2017**, *2*, 579–589; d) Ü. Kökçam-Demir, A. Goldman, L. Esrafili, M. Gharib, A. Morsali, O. Weingart, C. Janiak, *Chem. Soc. Rev.* **2020**, *49*, 2751–2798.

Manuscript received: November 18, 2022
Accepted manuscript online: February 9, 2023
Version of record online: February 24, 2023